



## Impact of Solid Core PCF Structure on SERS Performance

Zhigang Di<sup>1</sup>, Chunrong Jia<sup>2</sup>, Wenyuan Wang<sup>3</sup>

College of Electrical Engineering, Hebei United University, Tangshan Hebei 063009, China

### ABSTRACT

*The combination of photonic crystal fiber and surface enhanced Raman scattering sensor constructs photonic crystal fiber surface enhanced Raman scattering sensor, and this novel sensor has been given broad attention. The performance of this sensor will be affected by photonic crystal fiber's structure, substrates of surface enhanced Raman scattering and so on. To develop photonic crystal fiber surface enhanced Raman scattering sensor's huge action, the novel structure of solid core photonic crystal fiber was designed. On the base of ensuring fundamental transmission, increasing mode area is the most important. By numeral simulation, the designed solid core photonic crystal fiber has large mode area relative to other structures solid core photonic crystal fiber. So this structure photonic crystal fiber can ensure better surface enhanced Raman scattering performance*

**Key words:** Fiber optics Sensor; Photonic crystal fiber; SERS; FEM; mode area

### INTRODUCTION

It is well known that the development of low-loss optical fibers has greatly revolutionized the nature of optoelectronics owing to its various distinguished characteristics, including weak requirements for optical alignment, avoidance of free space laser beams, multiplexing, distributed sensing capabilities, and applicability for measurement applications in cramped, remote, and hazardous environments[1]. With the development of SERS, more and more scientists has tried to combined SERS and fiber sensor, namely fiber SERS sensor, and applied in chemistry and bios inspection [2-4]. This sensor has characteristics such as special molecule Raman scattering spectrum, huge SERS enhancement factor, and flexibility. The exciting light intensity and particles involved in SERS activity are dominant performance factors of SERS fiber sensor. To improve the performance, all kinds of different structure fiber such as tip-top fiber [4], D-fiber [5] was utilized as SERS inspection platform, but these fibers have not conquered the above two factors' confinement completely. While the air hole of PCF can provide large internal surface area for SERS effect, so PCF has been utilized as SERS platform to increase SERS action area, that is SERS PCF sensor.

The performance of this sensor will be affected by PCF's structure, substrates of SERS and so on. To improve it's performance, this paper proposed a novel solid core PCF, and gave the simulation result by finite element method. The result indicated that this kind of solid core PCF has large mode area, so can improve SERS PCF sensor performance remarkably.

### SERS EFFECT

SERS effect was first discovered by Jeanmaire[6] and Van Duyne[7] in 1977. Their result indicated that average Raman scattering section of each adsorbed pyridine molecule in rough silver electrode has an enhancement factor of 106 while the surface active area of rough silver electrode just increases by 10 times. This remarkable phenomenon is called SERS effect.

It is believed that three major mechanisms are responsible for SERS [8,9]: (a). Electro-magnetic enhancement

resulting from highly localized electro-magnetic fields in Plasmon resonance induced quasimetallic nanostructures. (b). chemical enhancement owing to the Raman molecules as the substrate, which leads to an increasing scattering cross section. (c). Geometrical enhancement as a result of the increase of surface area.

As to the main (a), (b) enhanced mechanisms, Kneipp K, et al[10] drew a conclusion that the intensity of SERS could be described as the following equation:

$$I_{SERS}(\nu_{SC}) = N' \cdot I(\nu_L) \cdot A^2(\nu_L) \cdot A^2(\nu_{SC}) \cdot \sigma_{adsorbed} \quad (1)$$

where  $I(\nu_L)$  is the intensity of incident light,  $N'$  is the number of active Raman molecules adsorbed by the enhanced substrates,  $\sigma_{adsorbed}$  is the scattering cross-section of chemical enhancement,  $A(\nu_L)$  and  $A(\nu_{SC})$  are the enhanced field amplitudes of incident light and scattering light, respectively.

Raman enhancement originates from enhanced electromagnetic fields localized at the metallic surface. The Stokes Raman signal is in proportion to the square of the intensity of local electromagnetic field, the surface area and the Raman scattering cross section. The number of Stokes photons per second can be written as[11]

$$P^{SERS} = \sigma_{ads}^S \frac{A}{A_0} \frac{|E_{loc}(\omega_i)|^2 |E_{loc}(\omega_R)|^2}{|E_0(\omega_i)|^2 |E_0(\omega_R)|^2} \quad (2)$$

where,  $\sigma_{ads}^S$  is the Stokes-Raman cross section of the adsorbed molecule,  $A/A_0$  is the ratio of the area of the

structured surface to the area of the unstructured surface and  $\frac{|E_{loc}(\omega_i)|^2 |E_{loc}(\omega_R)|^2}{|E_0(\omega_i)|^2 |E_0(\omega_R)|^2}$  describes the

electromagnetic enhancement factor, which results from the enhancement of the Raman radiation in a two-step-process: Firstly, the excitation of Raman-active molecules is in proportion to the square of the local electric field  $|E_{loc}(\omega_i)|^2 / |E_0(\omega_i)|^2$  at the incident frequency which can be very high on metallic surface. In the second step, the emitted Raman radiation is enhanced by the metal particle resonance which is in proportion to the local electric field at the Raman light frequency  $|E_{loc}(\omega_R)|^2 / |E_0(\omega_R)|^2$ . In most cases, the frequency of the Raman scattered light is close to that of the incident radiation so that the electromagnetic enhancement factor can be expressed as  $|E_{loc}(\omega_i)|^4 / |E_0(\omega_i)|^4$ .

Hence, to calculate the enhancement factor GSERS, taking into account the electromagnetic and geometric enhancement, the fourth power of the E-field amplitude is integrated and normalized over an unstructured surface.

$$G^{SERS} = \frac{1}{A_0} \int \frac{|E_{loc}|^4}{|E_0|^4} dA \quad (3)$$

This is an averaged enhancement factor assuming that the scattering molecules are distributed homogeneously over the substrate surface for most sensing applications.

In addition to the enhancement induced by the excitation of plasmonic dipoles, another mechanism based on an electrochemical process also contributes to the overall SERS intensity[23]. This mechanism relies on the fact that due to the charge transfer intermediate effect. The electron state of a molecule adsorbed on a metal surface will change accordingly. The new electron states act as resonant intermediates for the Raman radiation in a process is equivalent to Resonant Raman (RR) scattering.

SERS light has normally 6 to 11 orders of magnitude larger than Spontaneous Raman scattering light [23], which can be obtained by introducing closely packed nanoparticle ensembles such as fractals. In addition, it has been recently demonstrated that SERS offers exceptional sensitivity down to single molecule detection [24].

### SERS PCF SENSOR

Optical fiber SERS sensors have advantages of high sensitivity, interference-immunity, simple geometry, flexible light path and little analyte dependence, which ensures their potentiality in biochemical applications. Moreover, optical fiber SERS sensors lend themselves to single-ended measurement geometries, which are particularly attractive for minimally intrusive monitoring, such as in vivo biosensor and biomedical applications. Nowadays, metal nanoparticles have been utilized and developed widely as novel optics, electronics and magnetic materials [12,13]. The successful development of PCF made PCF combined with SERS sensor, formed novel sensor-SERS PCF sensor, and has been applied in chemistry, bios and circumstance inspection. The performance of SERS PCF sensor is determined by PCF structure, SERS substrates and so on, especially by PCF structure.

However, the confinement of preparation condition causes all kinds of bottlenecks in application. As a result, the numerical simulation on SERS PCF sensor's performance would be extremely valuable. Especially the numerical simulation is most instructive to prepare PCF. The numerical simulation on PCF was based on finite element method. To improve performance of SERS PCF sensor, the novel solid core PCF was designed by finite element method.

### SIMULATED MODELING

Solid core PCF is utilized to design SERS sensor, evanescent wave interacts with analytes involved in cladding air holes, so as to generate SERS signals. But solid core PCF SERS sensor has low sensitivity because mode area cannot interact with analytes adequately. It is highly important to design a novel solid core PCF to increase the action area between evanescent wave and analytes [14-17]. By theoretical analysis, increase mode area can meet this requirement. Besides, fundamental mode transmission at specific wavelength must be considered. The designed PCF must transmit exciting light as fundamental mode and has large mode area.

Based on this, a solid core PCF added six asymmetrically arranged between core and cladding air holes. The structure was displayed in Fig.1.

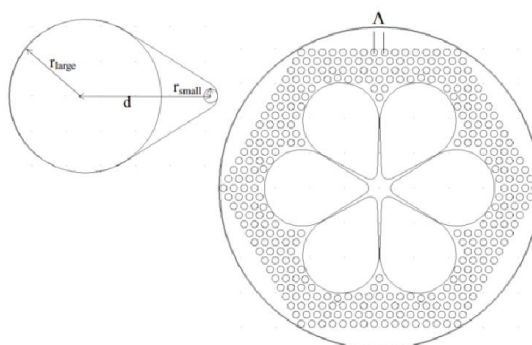


Fig.1: The structure of designed solid core PCF

This PCF was designed on the base of refractive index guided mode theory, so can utilize traditional numerical simulation to describe it. The six large air holes added between core and cladding air holes is better for filling analytes and metal nanoparticles, so can improve time response.

The design of this PCF was carried on in RF Module. The concrete parameters are as follows:  
 $r = 1\mu\text{m}$ ,  $\Lambda = 3\mu\text{m}$ ,  $r_{\text{large}} = 11\mu\text{m}$ ,  $r_{\text{small}} = 1\mu\text{m}$ ,  $d = 11\mu\text{m}$ .

### NUMERICAL SIMULATION

In this paper, the complex propagation constants of electromagnetic mode of the fiber sensor are investigated numerically via finite element method (FEM) with perfectly matched layer (PML) boundaries. When incident wavelength is 0.75  $\mu\text{m}$ , the power flow distribution of the sensor is presented as Fig. 2.

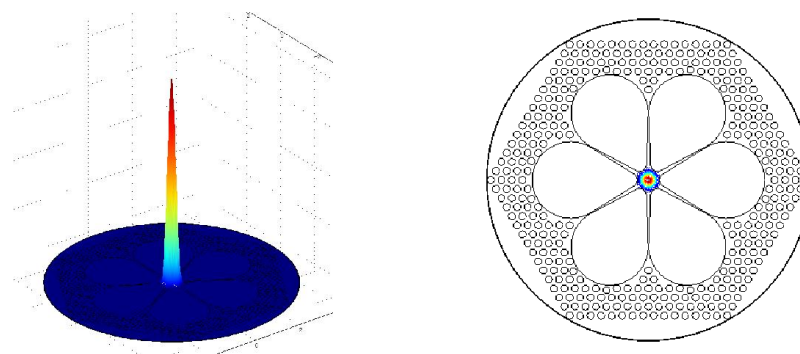


Fig.2: Electric field pattern of designed PCF

Dramatically, with the help of the auxiliary dielectric layer, most energy is transmitted in the core area of the PCF and only a part of the energy is leaked from the auxiliary dielectric layer to metal/dielectric interface to excite the SERS signal. The effective index  $n_{eff}$  is one of the most parameters, and it will change with transmission constant  $\beta$ , shown as formula (4)

$$n_{eff} = \frac{\beta}{k} = \frac{\lambda\beta}{2\pi} \quad (4)$$

As for the designed PCF,  $n_{eff} = 1.447727$ .

The PCF structure determines effective mode area ( $A_{eff}$ ), especially hole pitch and radius of cladding air holes and are decisive factors. As for PCF,  $A_{eff}$  can be calculated as formula (5)

$$A_{eff} = \frac{\left[ \iint |E(x, y)|^2 dx dy \right]^2}{\iint |E(x, y)|^4 dx dy} \quad (5)$$

As a result,  $A_{eff}$  can be calculated by the electric field distribution. And the integral function of post-processing can fulfill this job. To achieve better sensor performance,  $A_{eff}$  were calculated and compared for different  $r/\Lambda = 0.2 \sim 0.4$  and exciting wavelength  $\lambda = 0.45 \sim 0.8 \mu m$ , the result was shown in Fig.3.

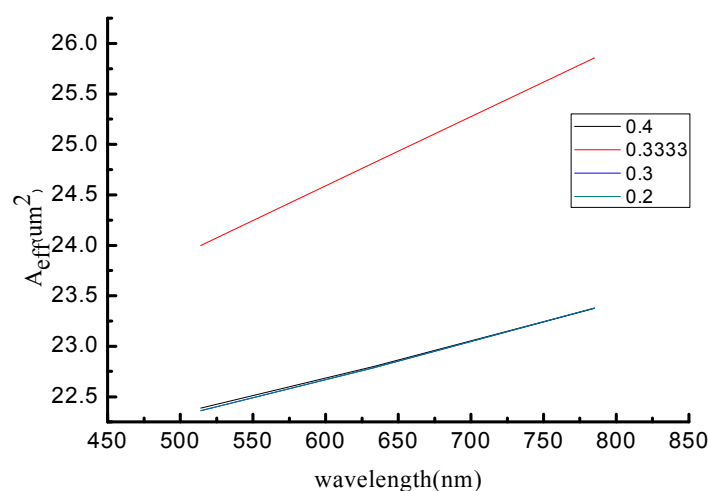


Fig.3:  $A_{eff}$  VS exciting wavelength for different

## CONCLUSION

Fig.3 indicated that  $A_{\text{eff}}$  varies directly with exciting wavelength for same  $r/\Lambda$ , and  $A_{\text{eff}}$  of  $r/\Lambda = 0.3333$  is more than other  $r/\Lambda$  for the same exciting wavelength, when exciting wavelength is 750 nm,  $A_{\text{eff}} = 25.6 \mu\text{m}^2$ . As a result, the designed PCF can excite more SERS signals.

This paper elaborated the influence of PCF structure on PCF SERS sensor performance. In order to improve the sensor's performance, the designed PCF must transmit exciting light as fundamental mode and has large mode area. Consequently, the PCF in which six large air holes were added between the core and cladding air holes was designed on the base of refractive index guided mode theory. Through numeral simulation of FEM, the designed PCF could transmit exciting light as fundamental mode at specific wavelength. Besides, this PCF has large mode area  $A_{\text{eff}} = 25.6 \mu\text{m}^2$ . More important, the designed PCF has six large air holes, which is better for filling analytes and metal nanoparticles, so can improve time response.

## Acknowledgments

This research was supported by scientific research fund of Hebei provincial education department(ZD2013102); in part by the Basic Research Program of Hebei province No. 12212172 and 12212201. Doctor Scientific Research Foundation of Hebei United University.

## REFERENCES

- [1] López-Higuera J M. *Handbook of optical fiber sensing technology [M]*. Wiley, Chichester, **2002**.
- [2] F.P. Kapron, D.B. Keck, R.D. Maurer. *Applied Physics Letters*, Vol. 17(10), pp. 423-425, **1970**.
- [3] C.L. Haynes, C.R. Yonzon, X. Zhang, et al. *Journal of Raman Spectroscopy*, Vol. 36(1), pp. 000-014, **2005**.
- [4] R. Gessner, P. Rosch, R. Petry, et al. *Analyst (Cambridge, U. K.)* Vol. 129(1), pp. 1193-1120, **2004**.
- [5] H.J. Feng, Y.M. Yang, Y.M. You, et al. *Chemical Communications*, Vol. 15(5), pp. 1984-1986, **2009**.
- [6] Y. Zhang, C. Gu, A.M. Schwartzberg, et al. *Applied Physics Letters*, Vol. 87(12), pp. 123105-123107, **2005**.
- [7] D.L. Jeanmaire, R.P. VanDuyne. *Journal of Electro analytical Chemistry and Interfacial Electrochemistry*, Vol. 84(1), pp. 1-20, **1977**.
- [8] M.G. Albrecht, J.A. Creighton. *Journal of the American Chemical Society*, Vol. 99(15), pp. 5215-5217, **1977**.
- [9] K. Kneipp, H. Kneipp, I. Itzkan, et al. *Journal of Physics: Condensed Matter*, Vol.14(4), pp. R597-R624, **2002**.
- [10] Martin Moskovits. *Rev. Mod. Phys.* Vol. 57(3), pp. 783-826, **1985**.
- [11] Kneipp K, Kneipp H, Itzkan I, et al. *Chemical Reviews*, Vol. 99(10), pp. 2957-2976, **1999**.
- [12] David P. Fromm, Arvind Sundaramurthy, Anika Kinkhabwala, et al. *The Journal of Chemical Physics*, Vol. 124(6), pp. 061101, **2006**.
- [13] Y. Zhu, H. Du, R. Bise. *Optics Express*, Vol. 14(8), pp. 3541-3546, **2006**.
- [14] T.M. Monro, W. Belardi, K. Furusawa, et al. *Measurement Science Technology*, Vol. 12(7), pp. 854-858, **2001**.
- [15] J.M. Fini. *Measurement Science Technology*, Vol. 15(6), pp. 1120-1128, **2004**.
- [16] Y. Zhang, C. Gu, A.M. Schwartzberg, et al. *Applied Physics Letters*, Vol. 87(12), pp. 123105, **2005**.
- [17] D. Pristiniski, H. Du. *Optics Letters*, Vol. 31(22), pp. 3246-3248, **2006**.